

INCREASED-ORDER AEROSERVOELASTIC MODELING IN PRACTICE

Manuel Reyes¹, Hector Climent¹, Moti Karpel², Felix Arévalo¹ and Carlos Maderuelo¹

¹ Airbus Defence & Space – Aeroelasticity and Structural Dynamics Department
Airbus, 28906 Getafe (Madrid), Spain
manuel.r.reyes@airbus.com, hector.climent@airbus.com, felix.arevalo@airbus.com,
carlos.maderuelo@airbus.com

² Faculty of Aerospace Engineering
Technion, Haifa 32000, Israel
moti_karpel@technion.ac.il

Keywords: structural dynamics, increased-order modeling.

Abstract: The inclusion of the Increased Order Modeling (IOM) methodology in the industry has provided means to address problems where concentrated non-linear effects of any kind are important while increasing the speed of standard aeroelastic calculations. This type of problems could only be addressed before by linearization techniques or by dedicated separated tools to approach each type of non-linearity.

This paper summarizes and details the following cases where this approach has been used at Airbus Defence & Space:

- Non-linear Flight Control System (FCS) in gust response.
- Non-linear boundary conditions in Aerial Refueling Boom System operation.
- Control surface freeplay induced loads calculation due to Limit Cycle Oscillation (LCO).
- Non-linear stiffness and rupture of elastomeric devices during a turbopropeller Blade Loss event.
- Non-linear aerodynamic forces.

Special attention is given to ease of implementation, robustness, calculation speed and upstream and downstream compatibility with the general dynamic loads calculation process.

1 INTRODUCTION

The methodology currently used to obtain the dynamic loads for aircraft design and certification typically relies on a linear formulation of the problem, which is based on the Finite Element Method to represent the structure and on the Doublet Lattice Method (DLM) to represent the unsteady aerodynamics. The advantages of this approach are: simplicity, robustness, efficiency (low CPU times) and the accuracy of the results.

Nevertheless, there are cases where the non-linear effects are of importance for loads, and the linearization is not easy, not accurate enough or not practical.

For instance, in the case of aircraft gust response with a non-linear Flight Control System, the problem was tackled in the past by linearization. The FCS was linearized and tuned to

produce the same loads as the ones obtained with slower, less robust, non-linear tools for a reduced set of cases, and it was then used for massive calculations.

Limit Cycle Oscillation loads induced by control surface freeplay, the rupture of elastomeric devices in a propeller Blade Loss event, or the contact of an Aerial Refueling Boom System with boundary conditions that change during its operation are examples where a concentrated structural non-linear effect plays a fundamental role in the response of the system. These dynamic scenarios have been usually studied using ad-hoc models and codes.

Increased Order Modelling provides a simple way of including these concentrated non-linear elements in the standard aeroservoelastic models and runs, simplifying the task and taking into account, if needed, unsteady aerodynamic forces calculated with frequency domain models.

2 INCREASED ORDER MODELLING IMPLEMENTATION: DYNRESP

Increased Order Modelling [1, 2] is based on the assumption that the aircraft is mainly linear and that the non-linear effects are concentrated and known, which is a reasonable hypothesis for many applications. The methodology has its roots in non-linear gust response calculation with non-linear Flight Control System. This problem, that is detailed in Section 4, perfectly fits to the requisites of having known and concentrated non-linear characteristics. The methodology has been expanded to other types of non-linearities (structural and aerodynamic) using the same tool with the same interfaces.

A general block diagram of the IOM calculation scheme is given in Figure 1. First, the linear aeroelastic core of the problem is solved in the frequency domain to obtain:

- The normal modes response to the excitation.
- The response to the excitation at the output towards the non-linear block (Y_{NL})
- The response at Y_{NL} to unitary excitations at the inputs from the non-linear block (U_{NL})

Then, these are transformed to time domain using Fast Fourier Transforms (FFT) and convolution integrals are used to solve the complete system.

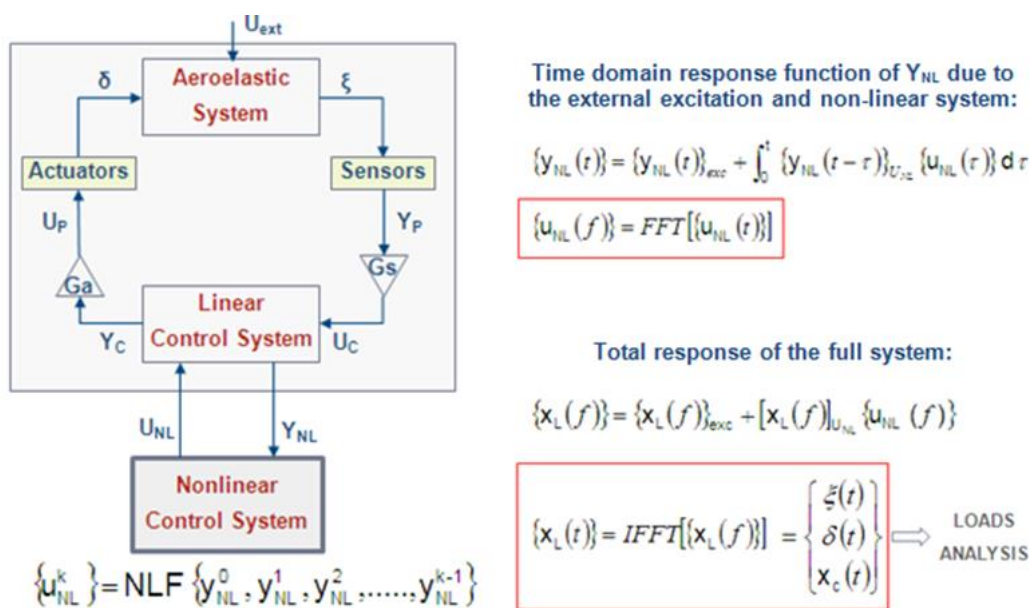


Figure 1: IOM calculation schema

The methodology has been implemented in the Dynresp code, which is the result of a fruitful collaboration between Karpel Dynamics Consulting and Airbus Defence & Space. It is a robust, fast, flexible and easy to use tool for aeroservoelastic calculations.

The development of Dynresp, besides solving the problems presented in this paper, has enabled different developments, such as solving the wake encounter problem in a very short period of time. Moreover, it has enabled to, not only integrate the tool in the loads calculation schema, but to improve it.

Figure 2 presents the solution schema of aeroservoelastic loads problems, both linear and non-linear: The dynamic model information, including geometry, modes, generalized mass and stiffness is obtained from MSC.Nastran solution 103 (Normal modes). Unsteady aerodynamic data is generally extracted from MSC.Nastran solution 146 (Aeroelastic response), although it can be obtained from other sources. Dynresp solves the aeroservoelastic equation, with or without non-linear elements, producing generalized coordinates time histories, which are input to the subsequent aircraft loads calculation code.

It can be noted that the normal modes calculation and the unsteady aerodynamic data extraction problems are decoupled, increasing the efficiency and flexibility of the solution schema.

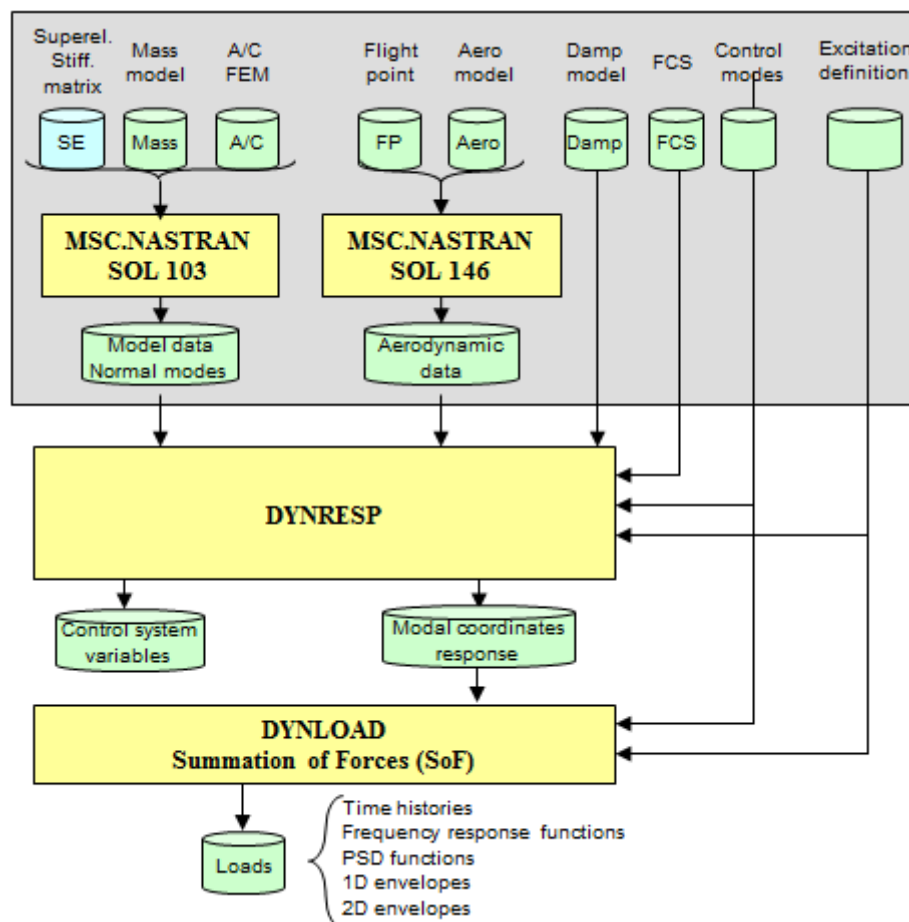


Figure 2: Aeroservoelastic response aircraft loads calculation schema

3 LINEAR CASE

The linear problem is solved in a very efficient manner, and this fact is key for the calculation speed of the non-linear analyses.

Figure 3 compares the calculation time of Dynresp vs. MSC.Nastran in a gust response problem [3]. It can be seen that the improvement is further increased when so does the amount of data (more subcases or smaller frequency step). Note that the Dynresp computation time includes the lapse used for modes and aerodynamic data calculation.

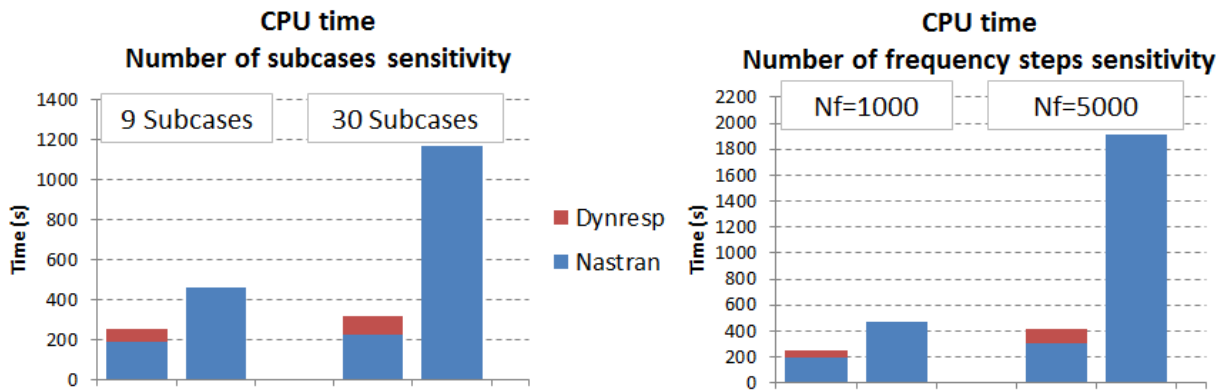


Figure 3: Linear runs calculation time comparison

4 NON-LINEAR FLIGHT CONTROL SYSTEM

4.1 Statement of the problem

Figure 4 represents a typical Flight Control System schema for longitudinal control, where aircraft variables are used to command control surfaces deflection. The Gust Loads Alleviation (GLA) system symmetrically deflects the ailerons when a gust is encountered in order to reduce the wing root bending moment.

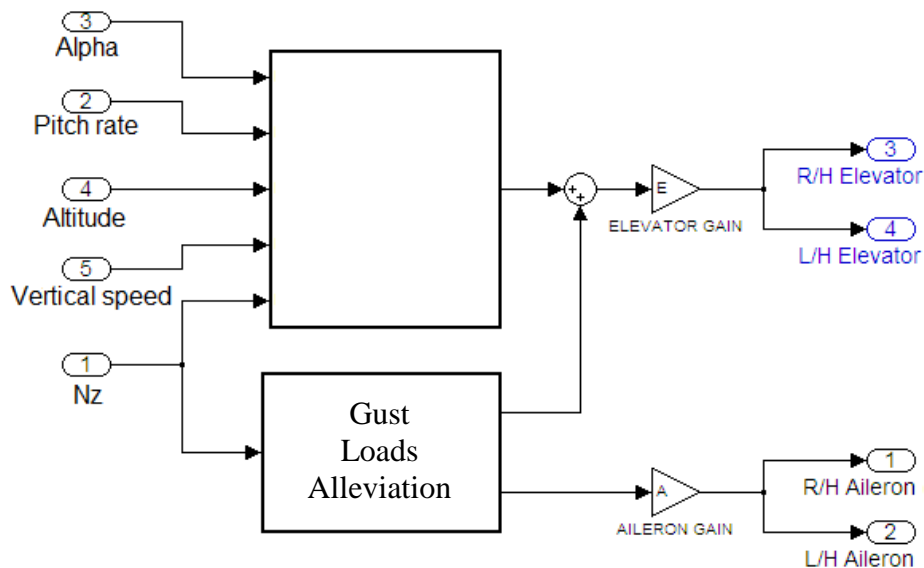


Figure 4: FCS schema

4.2 Identification of the non-linearity

The GLA is a very non-linear system that contains deflection and rate limiters, holds and look-up tables. For instance, the maximum aileron symmetric deflection (δ_{aileron}) commanded by the GLA as a function of the aircraft vertical acceleration (N_z) is presented in Figure 5.

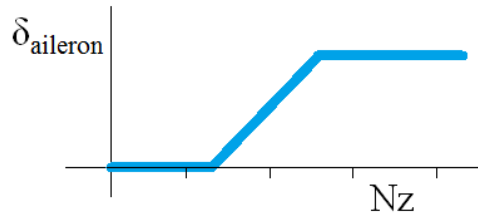


Figure 5: Maximum aileron deflection commanded by the GLA

These non-linear features have been treated before by a linearization and tuning process with the objective of producing the same loads as the ones obtained using alternative tools that were able to treat non-linear effects but were not practical for a complete loads loop in terms of robustness and CPU time.

4.3 Solution using IOM

The GLA has been implemented in Dynresp for gust loads calculation. In this case, the standard non-linear elements available in Dynresp have been used, mirroring the GLA schema, originally developed in Mathworks.Simulink.

The analysis yields similar results to the previous non-linear tools (Figure 6, left and center) but with CPU times comparable to the linear runs and therefore suitable for massive loads calculations (Figure 6, right).

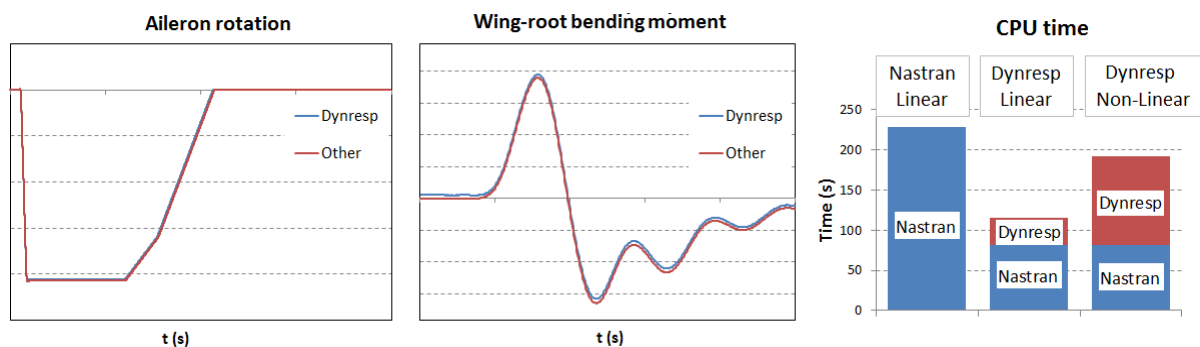


Figure 6: Non-linear flight control system discrete gust results

Technology Readiness Level for this application is TRL9.

5 NON-LINEAR BOUNDARY CONDITIONS IN AERIAL REFUELING BOOM SYSTEM OPERATION

5.1 Statement of the problem

The operation of the refueling boom on the A330-MRTT may lead the boom to go through different operation modes imposing different boundary conditions at the boom-to-aircraft fitting. This transition may induce important loads in some cases, as in the Safe Separation

Assessment (SSA) procedure, which is an evasive pitch-up that is performed to get a fast separation from the receiver aircraft in the event of any abnormal situation during the refueling operation.

5.2 Identification of the non-linearity

Figure 7 presents the A330MRTT with the extended boom during a refueling operation. The boom joint is detailed along with its two vertical rotation axes. The boom rotates around τ -mode axis when it is close to the stowage position, rotating around the γ -mode axis for the rest of attitudes.

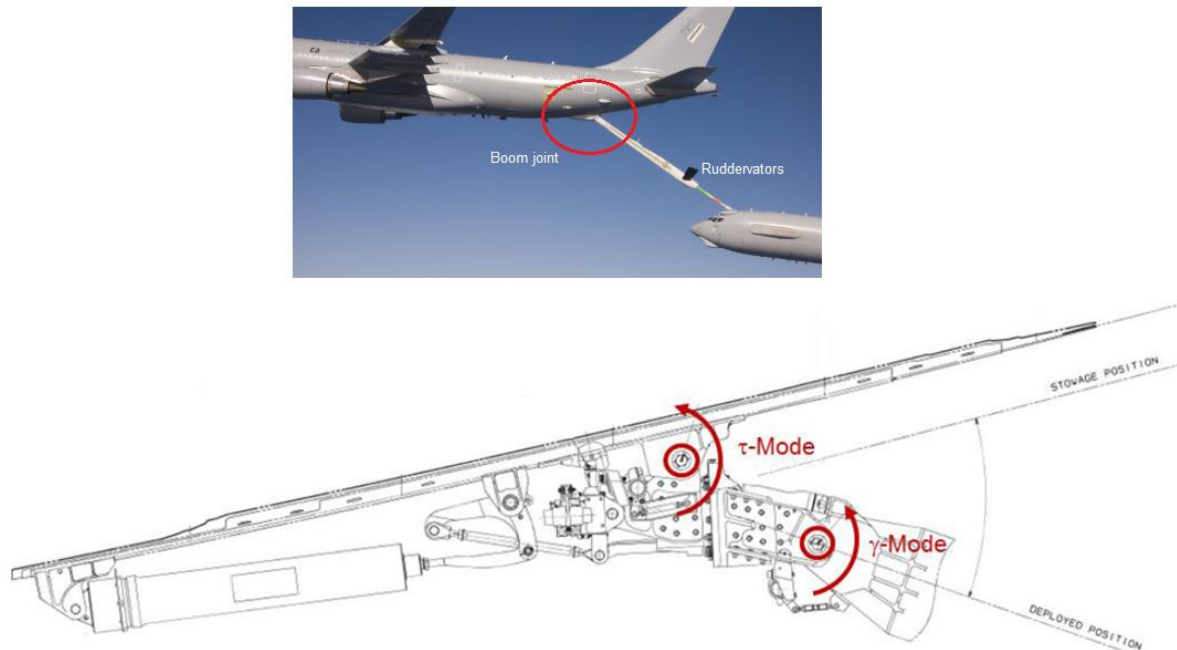


Figure 7: Boom joint. Actuation modes and angles

5.3 Solution using IOM

Figure 8 presents the loads calculation scheme. Model information is extracted from MSC.Nastran and provided to Dynresp (solver) and Dynload (loads calculation). The implementation of the boundary conditions was achieved in Dynresp by introducing positional sensors and feedback forces at the contact points applied while the contact is active.

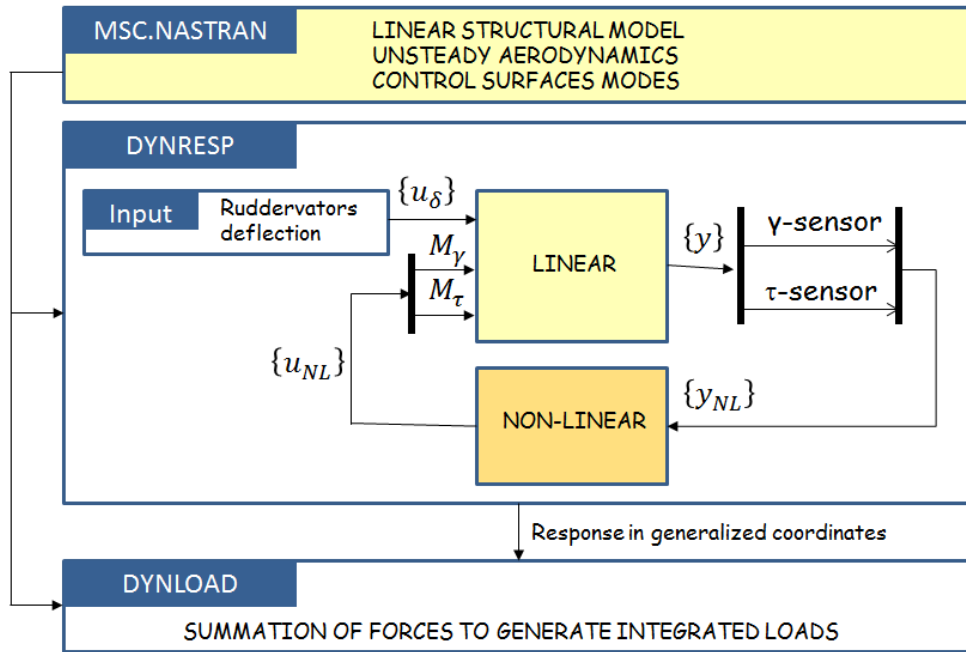


Figure 8: Boom SSA maneuver calculation scheme

The resulting accelerations were consistent with flight test, allowing for induced loads calculations. Figure 9 presents experimental and computed γ and τ angles, vertical acceleration at the boom head (N_z) and the boom root torque moment (M_x).

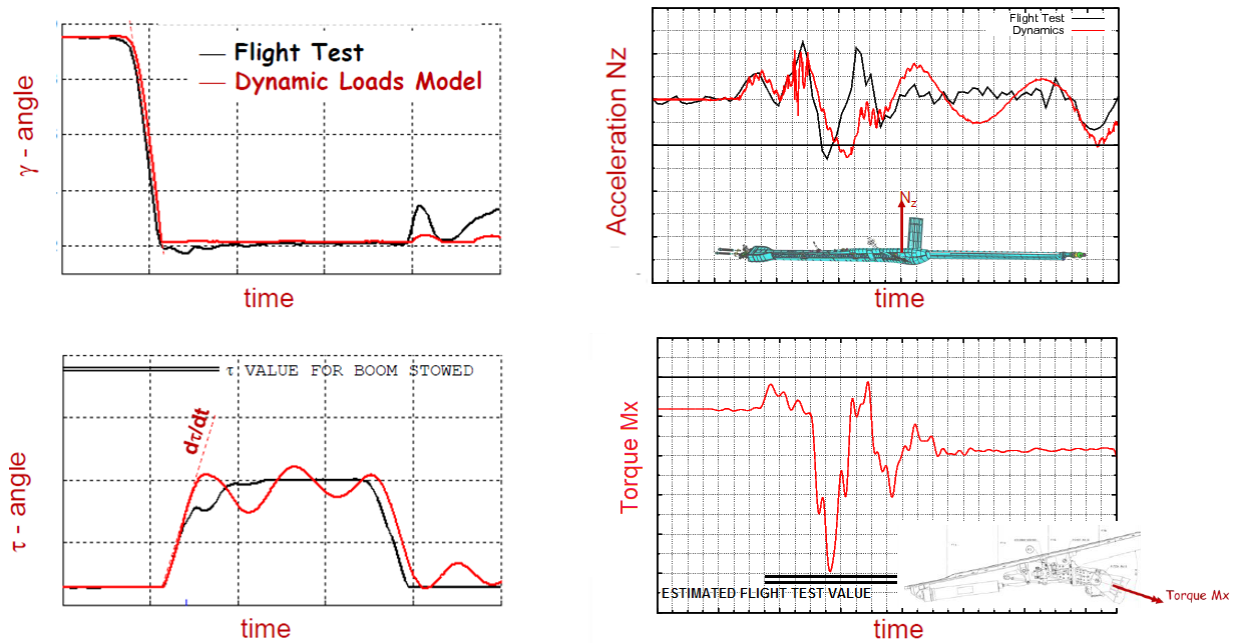


Figure 9: SSA maneuver simulation and validation

The calculation and validation of this case is detailed in [5].

Technology Readiness Level for this application is TRL8.

6 CONTROL SURFACE FREEPLAY INDUCED LOADS CALCULATION DUE TO LIMIT CYCLE OSCILLATION (LCO)

6.1 Statement of the problem

Aircraft control surfaces motion is generally driven by two actuators: the Servocontrol (S/C) actuator and the Electrohydrostatic (EHA) actuator.

- The S/C actuator is connected to the aircraft hydraulic lines and works in “active mode” which means that is actively governing the rotation of the control surface.
- The EHA actuator is not connected to the aircraft hydraulic lines and its own internal hydraulic pump is commanded electrically (“Power by wire”). The EHA actuator is usually in “damping mode” which means that is merely adding damping to the control surface motion. In addition, the EHA serves as backup actuator in case of S/C actuator failure, preventing from free-surface unbalanced flutter [3].

6.2 Identification of the non-linearity

While in active mode, the S/C actuator is represented by a spring with the adequate stiffness. The case shown here corresponds to a failure case where the S/C actuator is disconnected (its spring is removed) and the EHA has a freeplay stiffness-type in series with a damper (Figure 10).

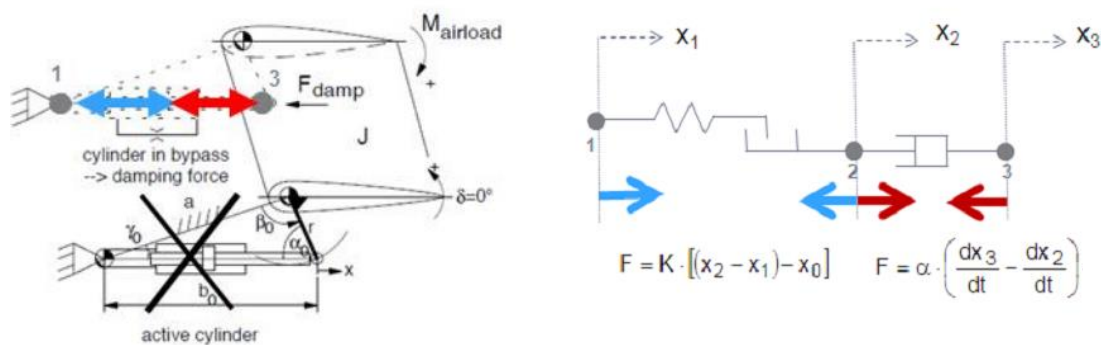


Figure 10: Elevator actuator failure mode scheme

6.3 Solution using IOM

This problem has been solved for the elevator of a heavy cargo aircraft using Dynresp, as indicated in Figure 11. The initial model corresponds to the actuator failure case, where the springs modeling the actuators are removed. Generalized stiffness and mass matrices, normal modes, model geometry and unsteady aerodynamic data is extracted using MSC.Nastran.

The Dynresp run starts by adding the springs modeling the actuators to create the linear plant. The gust is used to trigger the response.

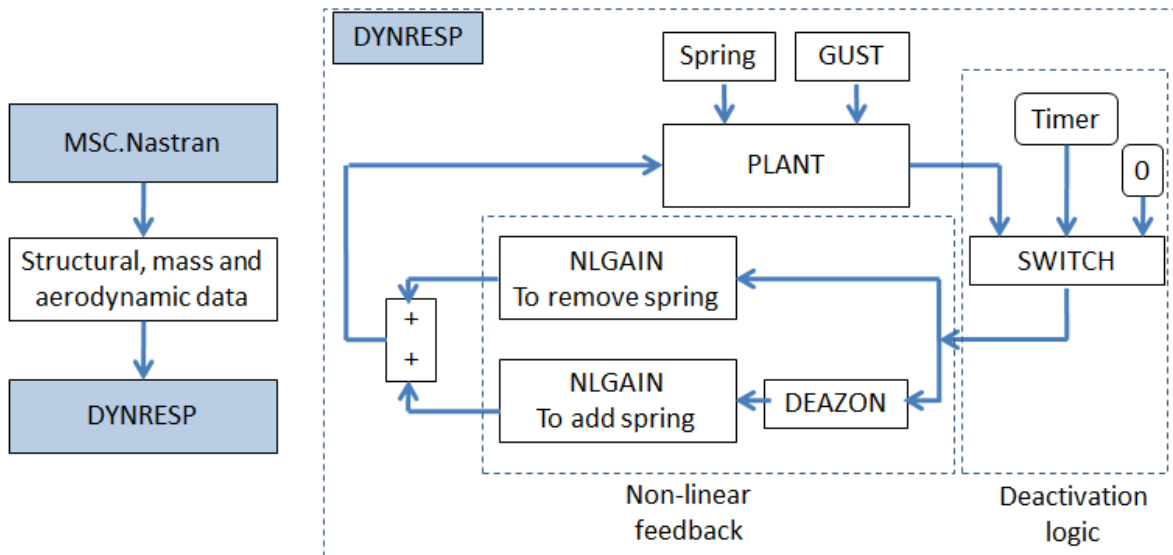


Figure 11: LCO response calculation schema

To simulate the actuator failure, a non-linear feedback loop is added so that the resulting stiffness (springs + non-linear feedback) reproduces the freeplay behavior (Figure 12), similarly to the LCO analysis in Ref [6].

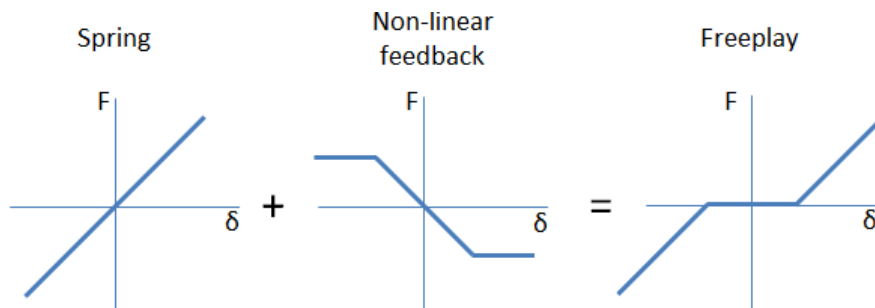


Figure 12: Freeplay modelization schema

Once the input from the non-linear part of the solution is calculated in the time domain, it is transformed to the frequency domain using FFT. For this, the response should start and end at the same value, i.e. the response must be periodic. The simulation result, however, is a LCO that will not return to the initial rest situation. To ensure that the system response is at rest at the end of the calculation period, a deactivation logic is introduced so that after 20 seconds the non-linear forces are set to zero. With zero feedback forces, the LCO is stopped and the response decays to zero, fulfilling the periodic condition.

Figure 13 presents the elevator actuator elongation time history.

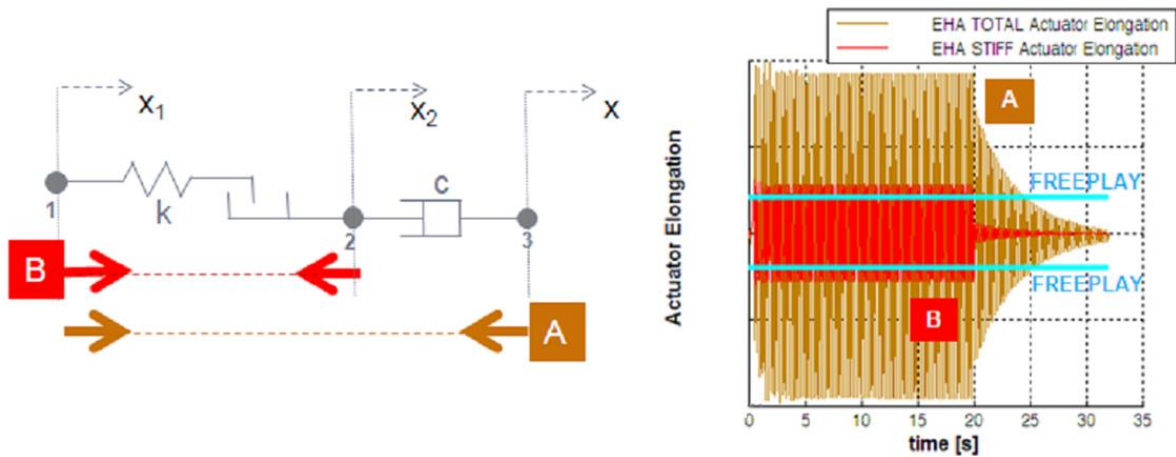


Figure 13: LCO. Actuator elongation time history

Technology Readiness Level for this application is TRL6.

7 NON-LINEAR STIFFNESS AND RUPTURE OF ELASTOMERIC DEVICES DURING TURBOPROPELLER BLADE LOSS EVENT

7.1 Statement of the problem

During a turbopropeller blade loss event, high loads are produced at the propeller hub due to mass imbalance (Figure 14).

The present study aims at simulating the rupture sequence of the isolators that link the engine to the nacelle, continuing the work initiated in [3]. A medium cargo aircraft dynamic model has been used, consisting in half structural and mass models, with detailed wing, nacelle and HTP, and condensed fuselage, engine and VTP (Figure 14). The imbalance load is simulated by introducing a rotating load applied at the propeller hub.

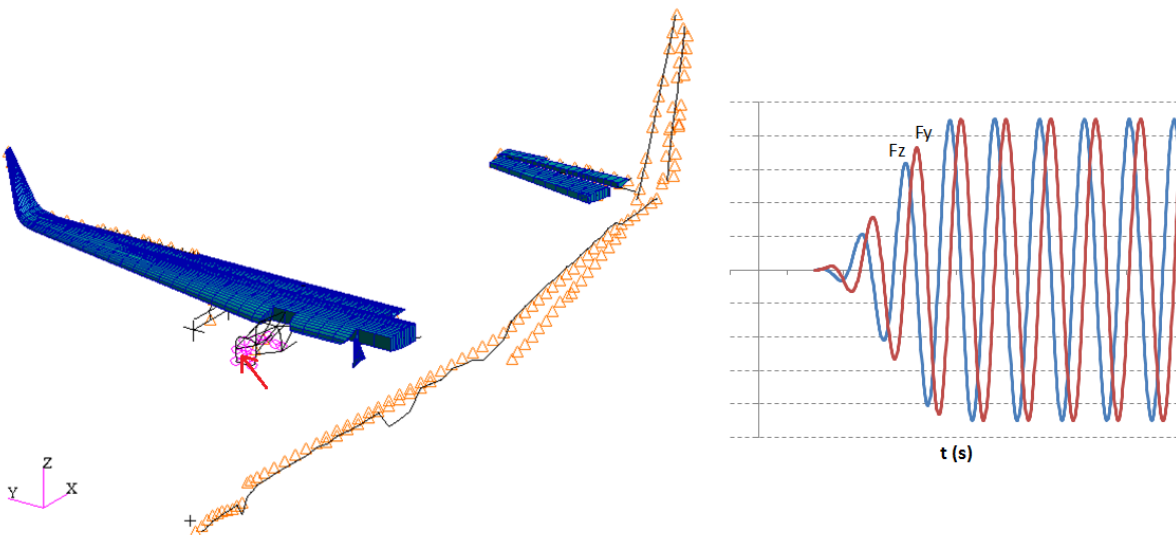


Figure 14: Aircraft FEM and imbalance load time history

7.2 Identification of the non-linearity

The imbalance loads are transmitted to the engine, and then to the nacelle structure through a set of flexible elastomeric isolators (Figure 15). The isolators may reach rupture when their deformation exceeds certain limits.

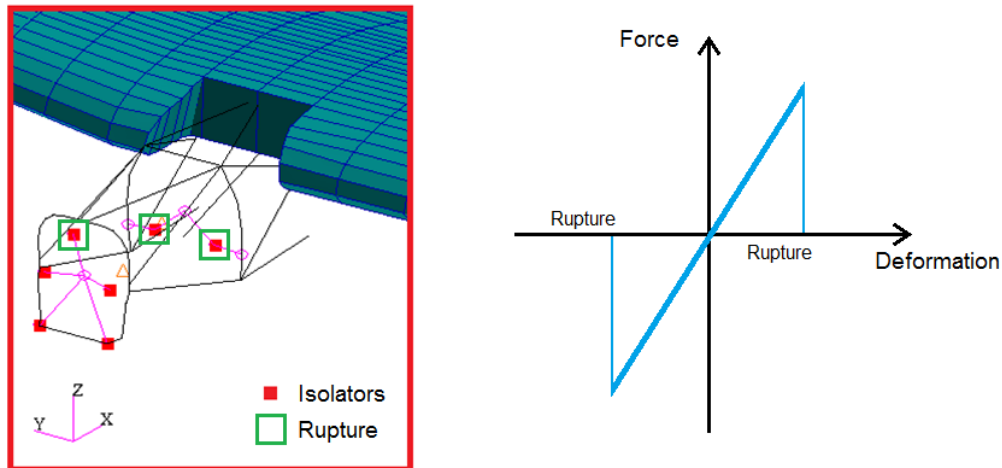


Figure 15: Isolators location and rupture

In the present analysis, a step-by-step approach is followed, studying two configurations:

- Rupture of the rear isolators (left and right)
- Rupture of the rear (left and right) and front top isolators.

The failure effects on the main engine natural frequencies in each case are presented in Figure 16. Note that the rupture of the rear and front top isolators produce a zero frequency engine pitch mode.

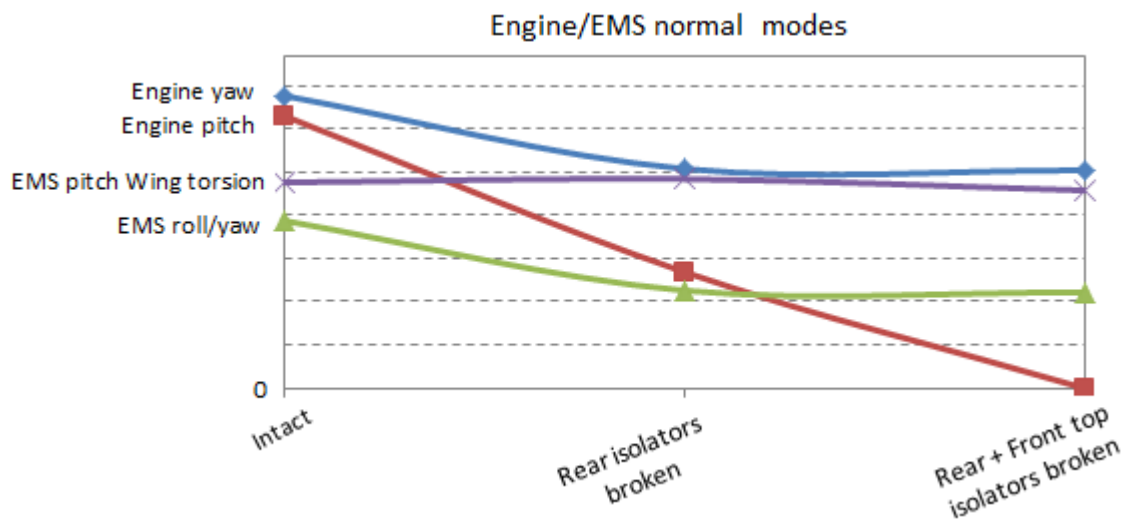


Figure 16: Engine and EMS natural frequencies variations

7.3 Solution using IOM

In a similar manner to Section 6, the modal base with the broken isolators is used. The nominal stiffness of the isolators is introduced in Dynresp before the analysis using springs so

that the model behaves as the intact one at the beginning of the run. During the response analyses, this stiffness is removed when the rupture limit of an isolator is reached using a user-defined non-linear element, referred here as Rupture. This demonstrates an important feature of Dynresp, which accommodates nonlinear feedback elements that are programmed by the user.

The developed Rupture element has 4 inputs and 4 outputs. The inputs are the sensors measuring the deformation of the isolator in 3 directions plus the simulation time. The first three outputs are zero if the isolator is not broken, and are equal to the inputs when the rupture limit is reached and until a user defined analysis instant is reached. This last feature has been introduced to deactivate the non-linear feedback force before the end of the analysis, which is necessary in case the rupture of the isolators lead to an unstable system. The fourth output (“Control” in Figure 17) monitors whether the isolator is broken or not. Different limits may be introduced in each deformation direction. The implementation schema for one isolator is presented in Figure 17. With this element, it is considered that when the rupture limit is reached in one direction, the complete isolator breaks. Note that the objective of this element is to remove the stiffness of the broken element. It is not a structural element that can break.

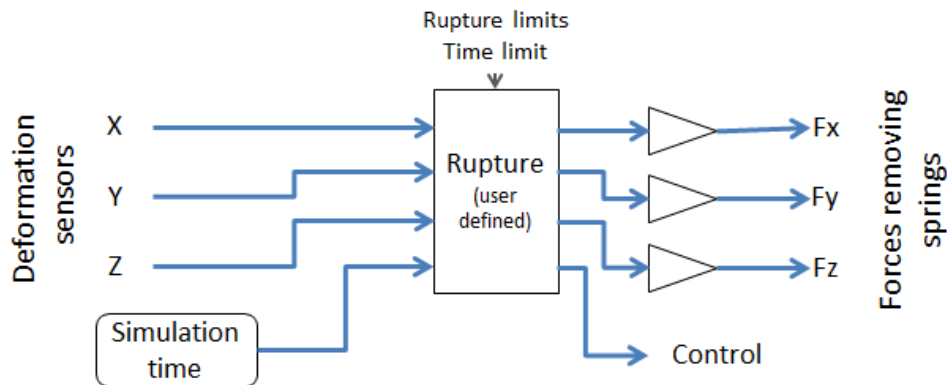


Figure 17: Isolator rupture modelization schema

The response of the system is represented by the deformation time histories of the involved isolators. Figure 18 presents, for the configuration where only the rear isolators may break, the results for the rear left isolator. While the deformation is below the rupture limits, the response (plotted in blue) matches the one obtained with the linear intact model (red curve). The limit is reached first at the left isolator in the Y direction, followed very shortly by the right one. The non-linear feedback forces applied are shown in Figure 19.

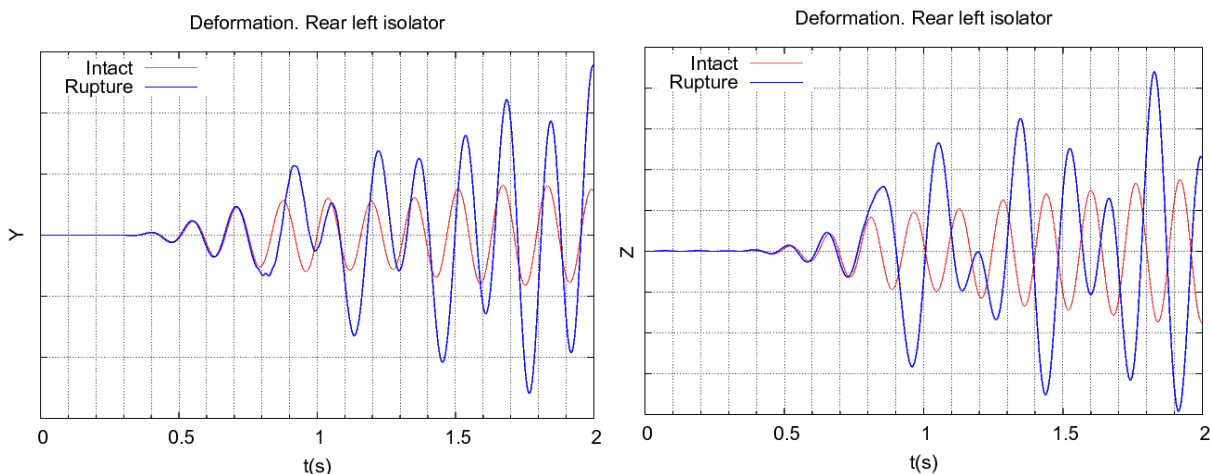


Figure 18: Rear left isolator response for rear isolators rupture

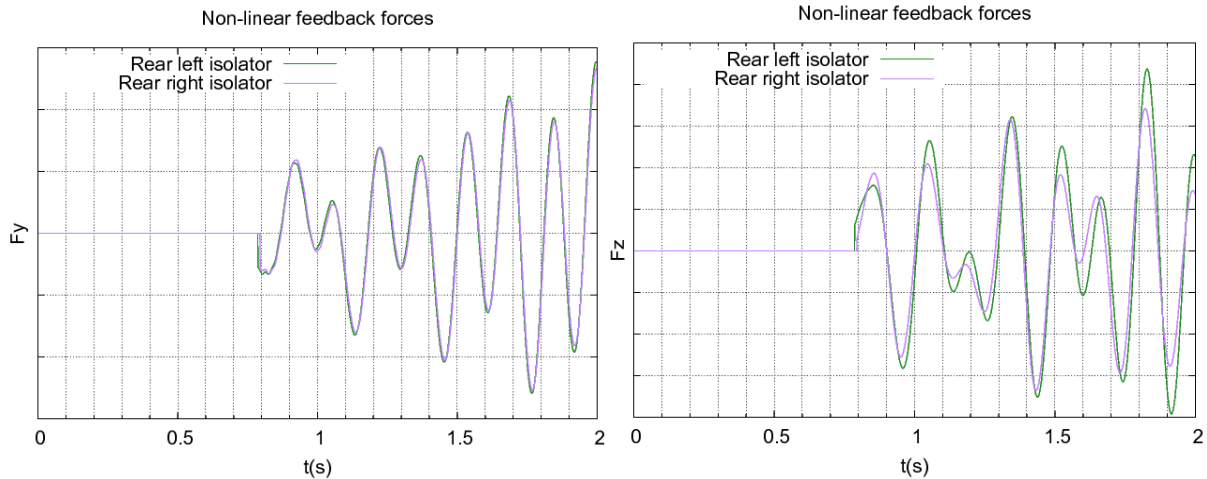


Figure 19: Non-linear feedback forces for rear isolators rupture

It is interesting to note that once the imbalance load has been stopped but while the non-linear forces are still acting, the frequency analysis of the response shows a peak at the Engine pitch mode of the broken model (Figure 20). Once the feedback force is stopped, the response is the one of the intact model, as before the rupture is reached.

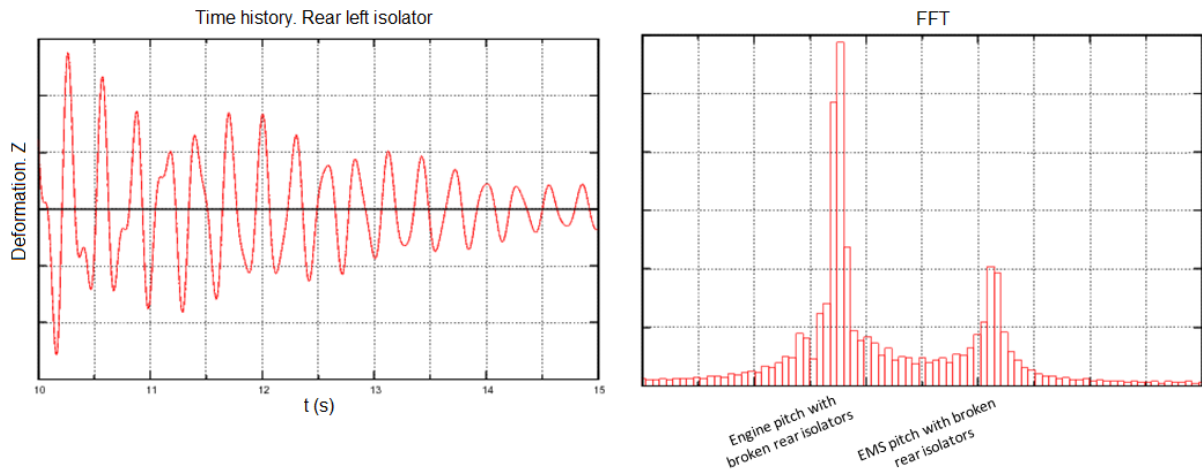


Figure 20: Time history and FFT of the broken model free response.

In the second configuration studied, the rear and the front top isolators may reach rupture. Again, before reaching the rupture limits, the response matches the linear intact model. The first elements to break are the rear isolators, followed by the front top one (Figure 21, Figure 22).

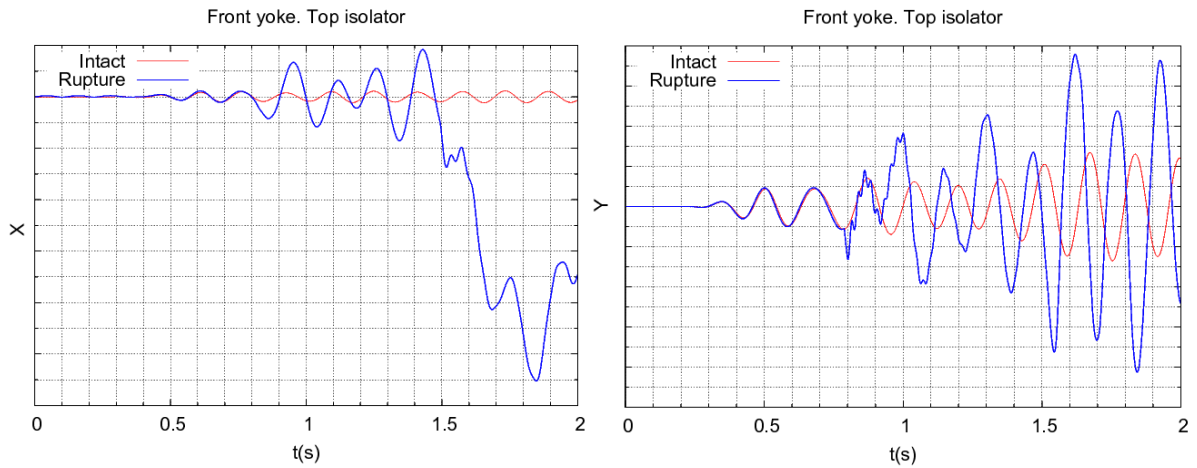


Figure 21: Front top isolator response for rear + front top isolators rupture

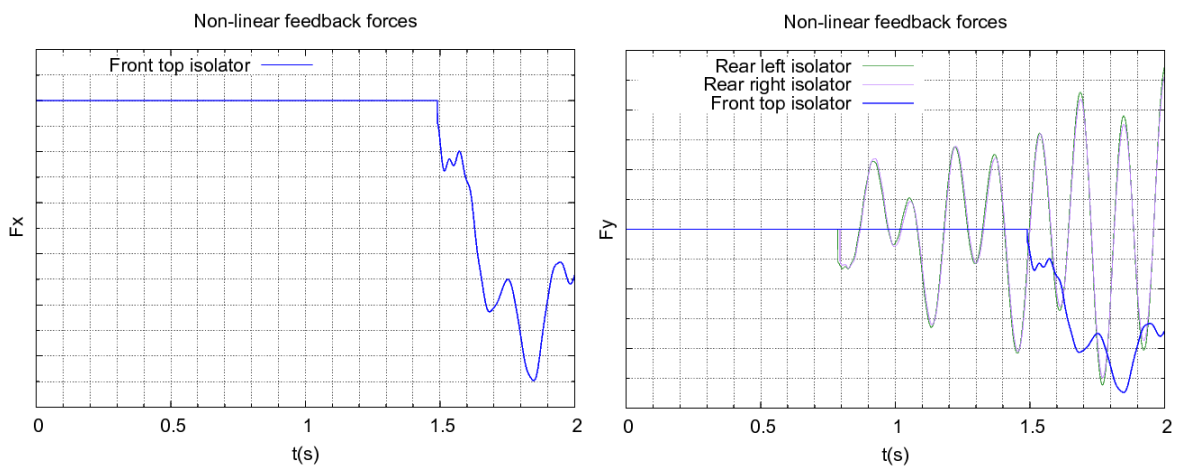


Figure 22: Non-linear feedback forces for rear + front top isolators rupture

Once the front top isolator breaks the system response changes completely, as can be seen in a wider view in Figure 23.

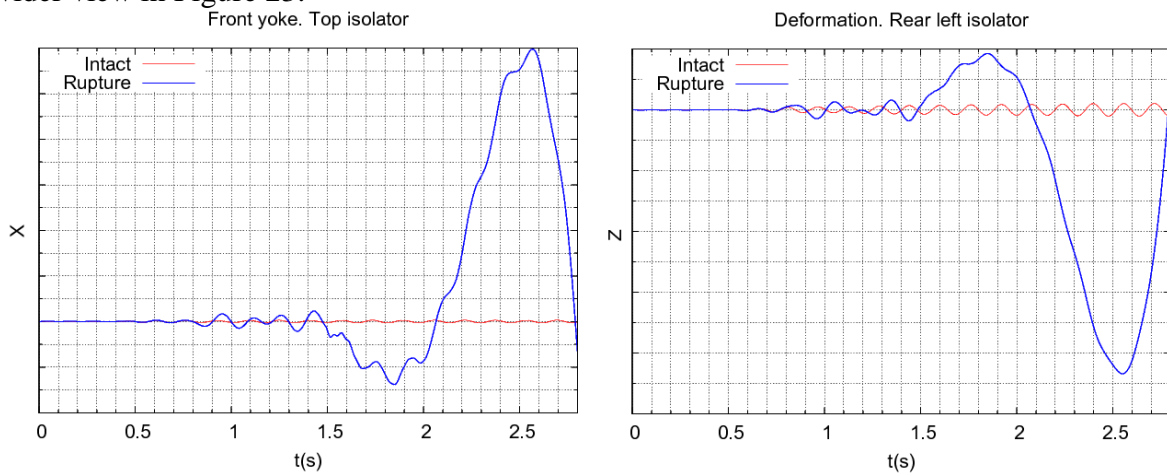


Figure 23: Isolators deformation for rear + front top isolators rupture. Wide view

Technology Readiness Level for this application is TRL6.

8 NON-LINEAR AERODYNAMIC FORCES

8.1 Statement of the problem

The aim of this section is to implement and test the virtual aerodynamic sensors feature in Dynresp. It can be of two types:

- Angle of attack sensor.
- Aerodynamic forces sensor.

The first type can be used, for instance, to introduce non-linear angle of attack depending forces or to serve as input to a FCS. The second type is used in this paragraph to demonstrate its use in a simple example where the lift coefficient is limited to 0.2 during gust response.

8.2 Solution using IOM

The wing unsteady aerodynamic model has been divided in 28 strips, as shown in Figure 24.

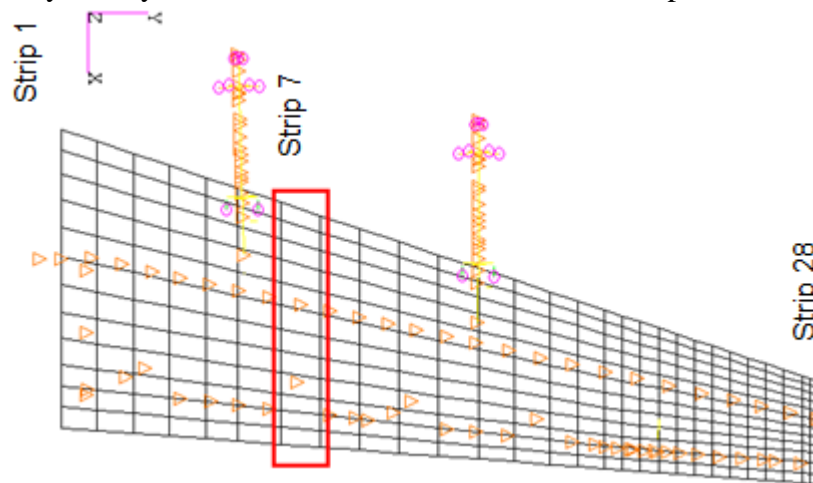


Figure 24: Aerodynamic model layout showing one of the aerodynamic sensors

For each strip, a sensor has been implemented to measure its aerodynamic forces. This signal is input to a non-linear element that generates a force applied to the structure to counter act the aero forces and in practice limit the forces introduced by the aerodynamic model (Figure 25).

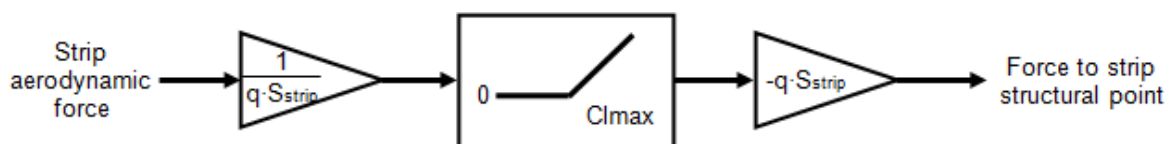


Figure 25: Aerodynamic force feedback loop example

Figure 26 presents the results of the gust response simulation. On the left, the lift spanwise distribution is presented with and without the non-linear feedback loop. In the center, the impact on wing loads is presented to highlight Dynresp compatibility with subsequent loads calculation tools.

Again, the CPU calculation time shown on the right side is compatible with industrial requirements as is comparable to the linear gust response.

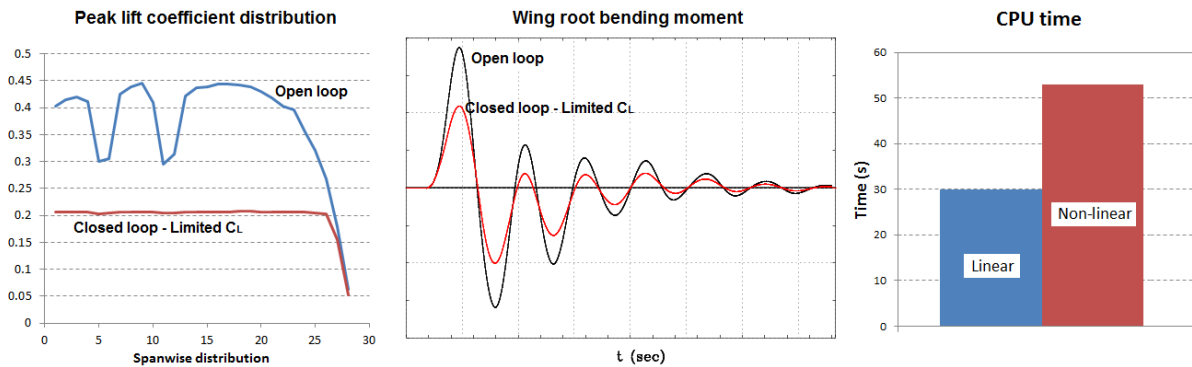


Figure 26: Non-linear control based on aerodynamic sensors results

Technology Readiness Level for this application is TRL3

9 CONCLUSION

During the last years, Increased Order Modeling methodology and its implementation in the Dynresp code, have been introduced in Airbus Defence & Space as the standard tool for aeroservoelastic dynamic loads calculations. While not completely replacing the previous codes, as it relies on them for model data extraction, validation and specific tasks, the tool improves significantly the calculation speed and permits to tackle problems that were formerly solved with ad-hoc slower tools, as for instance, problems in which the non-linear behavior plays an important role.

The Dynresp code fits seamlessly with the standard loads calculation methodology and permits to implement control, structural and aerodynamic non-linearities in a standardized manner.

Future developments will continue to improve on the structural non-linear elements case, non-linear aerodynamics and geometrical non-linearities.

10 REFERENCES

- [1] P. Teufel, M. Kruse. "Efficient Method for Coupling Discrete Gust Loads Analysis in the Frequency Domain with a Fully Non-Linear Flight Control System Simulation" Proceedings of the International Forum of Aeroelasticity and Structural Dynamics, Stockholm, June 18-20 2007
- [2] Karpel, M., Moulin, B., Presente, E., Anguita, L., Maderuelo, C., and Climent, H., "Dynamic Response to Gust excitation with Non linear Control Systems", Proceedings of the International Forum of Aeroelasticity and Structural Dynamics, IFASD 2007, Stockholm. 18 – 20 June 2007.
- [3] Maderuelo C., Pérez de la Serna A., Reyes M. "Increased Order Modeling for Non-linearities in Dynamic Loads". EADS Workshop on Aeroelasticity and Structural Dynamics (June 2012).
- [4] Karpel, M., Present, E., Anguita, L., Maderuelo, C., and Climent, H. "Gust Loads on Transport Aircraft with Nonlinear Control System", 48th Israel Annual Conference on Aerospace Sciences. Technion, Haifa, 27-28 February 2008.

- [5] Arévalo F., Claverías S. and Climent H. “Non-Linear Structural Dynamics aspects of the Aerial Refuelling Boom System”. International Forum of Aeroelasticity and Structural Dynamics. Saint Petersburg, Russia (June 28-July 02, 2015)
- [6] Karpel M., Shousterman A., Maderuelo C. and Climent H. “Dynamic aeroservoelastic response with nonlinear structural elements” AIAA Journal, Vol. 53, No. 11, 2015, pp. 3233-3239

COPYRIGHT STATEMENT

The authors confirm that they, and/or their company or organization, hold copyright on all of the original material included in this paper. The authors also confirm that they have obtained permission, from the copyright holder of any third party material included in this paper, to publish it as part of their paper. The authors confirm that they give permission, or have obtained permission from the copyright holder of this paper, for the publication and distribution of this paper as part of the IFASD-2017 proceedings or as individual off-prints from the proceedings.